AD-A162 027 NONLINEAR FRACTURE MECHANICS ANALYSIS WITH THE BO_NDARY 1/1
INTEGRAL METHOD(U) SOUTHWEST RESEARCH INST SAN ANTONIO
TX T A CRUSE ET AL 30 APR 85 AFOSR-TR-85-1072
UNCLASSIFIED F49620-84-C-0042 F/G 20/11 NL

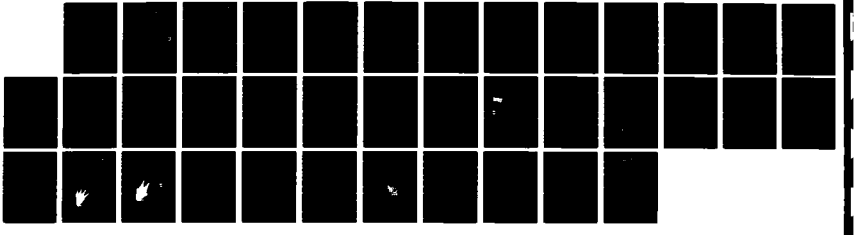

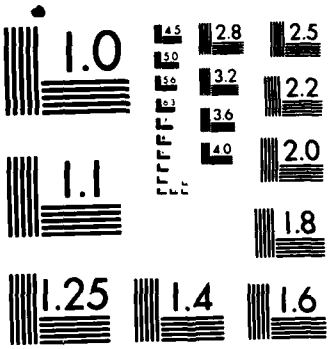

(1)

NONLINEAR FRACTURE MECHANICS ANALYSIS WITH THE BOUNDARY INTEGRAL METHOD

by
T. A. Cruse
E. Z. Polch

ANNUAL TECHNICAL REPORT
SwRI Project No. 06-8044

for
Air Force Office of Scientific Research
Washington, D.C. 20332

April 30, 1985

SOUTHWEST RESEARCH INSTITUTE
SAN ANTONIO HOUSTON

UNCLASSIFIED

URITY CLASSIFICATION OF THIS PAGE

AD-A162 027

REPORT DOCUMENTATION PAGE

REPORT SECURITY CLASSIFICATION Unclassified	1b. RESTRICTIVE MARKINGS
SECURITY CLASSIFICATION AUTHORITY	3. DISTRIBUTION/AVAILABILITY OF REPORT Approved for public release; distribution unlimited.
DECLASSIFICATION/DOWNGRADING SCHEDULE	Unlimited Distribution
ERFORMING ORGANIZATION REPORT NUMBER(S) 06-8044	5. MONITORING ORGANIZATION REPORT NUMBER(S) AFOSR-TR- 85-1072
NAME OF PERFORMING ORGANIZATION Southwest Research Institute	6b. OFFICE SYMBOL (If applicable)
	7a. NAME OF MONITORING ORGANIZATION Air Force Office of Scientific Research
ADDRESS (City, State and ZIP Code) P. O. Drawer 28510 San Antonio, Texas 78284	7b. ADDRESS (City, State and ZIP Code) Bolling Air Force Base Washington, D. C. 20332
NAME OF FUNDING/SPONSORING ORGANIZATION AFOSR	8b. OFFICE SYMBOL (If applicable) AFOSR/NA
	9. PROCUREMENT INSTRUMENT IDENTIFICATION NUMBER Contract No. F49620-84-C-0042
ADDRESS (City, State and ZIP Code)	10. SOURCE OF FUNDING NOS.

PROGRAM ELEMENT NO.	PROJECT NO.	TASK NO.	WORK UNIT NO.
61102F	2302	B2	

TITLE (Include Security Classification)
NONLINEAR FRACTURE MECHANICS ANALYSIS WITH THE BOUNDARY INTEGRAL METHOD

PERSONAL AUTHOR(S)
T. A. Cruse and E. Z. Polch

TYPE OF REPORT	13b. TIME COVERED	14. DATE OF REPORT (Yr., Mo., Day)	15. PAGE COUNT
Annual Research	FROM 4/2/84 TO 3/29/85	1985 April 30	31

SUPPLEMENTARY NOTATION

COSATI CODES		
ELD	GROUP	SUB. GR.

18. SUBJECT TERMS (Continue on reverse if necessary and identify by block number)
Fracture mechanics, two dimensions, elastoplasticity, computational methods, fatigue crack growth, damage tolerance

ABSTRACT (Continue on reverse if necessary and identify by block number)

The current research makes use of the boundary integral equation (BIE) method, as modified to account exactly for the elastic crack problem. The usual BIE formulation for elastic problems reduces the numerical problem to one of modeling the boundary data, while preserving the complete interior solution of the field equations. In the elastic fracture mechanics problem, the Green's function approach is used wherein the BIE is modified to account for the presence of a stress free crack at an arbitrary location within the structure. The use of the Green's function for the crack eliminates the need to model the boundary of the crack, and provides a complete mathematical description of the elastic strain field within the body, due to the crack. This clearly contrasts with the finite element method which requires that the crack surface and the interior strains be modeled with some set of interpolation functions.

DISTRIBUTION/AVAILABILITY OF ABSTRACT	21. ABSTRACT SECURITY CLASSIFICATION
CLASSIFIED/UNLIMITED ☒ SAME AS RPT. ☐ DTIC USERS ☐	Unclassified

NAME OF RESPONSIBLE INDIVIDUAL	22b TELEPHONE NUMBER (Include Area Code)	22c. OFFICE SYMBOL
Major David Glasgow	202/767-4987	Directorate of Aerospace Sciences

FORM 1473, 83 APR EDITION OF 1 JAN 73 IS OBSOLETE.

UNCLASSIFIED
SECURITY CLASSIFICATION OF THIS PAGE

19. (Continued)

The BIE method has been successfully modified to account for elastoplastic response by a number of investigators. However, extension of the fracture mechanics model with the Green's function approach has not been previously demonstrated. In order to account for elastoplastic response with the BIE method one must numerically model the interior plastic strain field. In all other ways the elastoplasticity solution uses the standard elastic BIE formulation. The current work reports on the successful extension of the special Green's function formulation for the fracture mechanics problem to the elastoplasticity formulation. Not only has the work resulted in accurate models of crack tip plasticity for a reference problem, but it has shown some important new analytical and numerical results for cracks growing in plastic strain fields.

Table of Contents

List of Tables

List of Figures

INTRODUCTION

The effect of plasticity on the rate of growth of fatigue cracks is significant for a wide range of problems associated with the damage tolerance assessment of aerospace structures. The range of problems includes crack growth from cold worked fastener holes, crack growth through plasticity due to local notch stresses, crack driving force for thermal gradient fields and welding residual strain fields, small flaw growth in high nominal stress fields, and numerous related problems. These problems have, of course, been analyzed using a variety of approximate analytical or numerical procedures. However, as will be summarized within this report, many of these earlier modeling approaches have involved errors which may significantly affect the predicted fatigue crack growth life of the structure. The current research has resulted in some new and critical insights into this class of problems, while providing a basis for improved modeling of these problems.

The current research makes use of the boundary integral equation (BIE) method, as modified to account exactly for the elastic crack problem. The usual BIE formulation for elastic problems reduces the numerical problem to one of modeling the boundary data, while preserving the complete interior solution of the field equations. In the elastic fracture mechanics problem, the Green's function approach is used wherein the BIE is modified to account for the presence of a stress free crack at an arbitrary location within the structure. The use of the Green's function for the crack eliminates the need to model the boundary of the crack, and provides a complete mathematical description of the elastic strain field within the body, due to the crack. This clearly contrasts with the finite element method which requires that the crack surface and the interior strains be modeled with some set of interpolation functions.

The BIE method has been successfully modified to account for elastoplastic response by a number of investigators. However, extension of the fracture mechanics model with the Green's function approach has not been previously demonstrated. In order to account for elastoplastic response with the BIE method one must numerically model the interior plastic strain field. In all other ways the elastoplasticity solution uses the standard elastic BIE formulation. The current work reports on the successful extension of the special Green's function formulation for the fracture mechanics problem to the elastoplasticity formulation. Not only has the work resulted in accurate models of crack tip plasticity for a reference problem, but it has shown some important new analytical and numerical results for cracks growing in plastic strain fields.

The second year of the contract effort will focus on the crack growth problem. That is, the effect of crack tip plasticity on the subsequent crack growth rate will be studied. The effects of crack tip overloads on retardation or acceleration through closure and residual stress effects will be studied. In addition, the elastoplastic BIE formulation will be more fully exploited for problems of crack growth in residual strain and thermal strain fields. The purpose of all of these studies will be to identify modeling shortcomings in current practice for these problems as well as to provide some new results for the small flaw problem.

RESEARCH OBJECTIVES

Generally speaking, advanced aerospace structures have been designed for damage tolerance considerations using elastic fracture mechanics models. Problems associated with residual plastic strains at notches, cold worked fastener holes, weld residual strains, and thermal gradient loading have been modeled using elastic superposition methods along with elastic fracture mechanics models. Crack tip plasticity is involved in all fatigue crack growth problems. Crack tip plasticity dominates the problem of predicting crack growth under spectrum loading conditions where acceleration and retardation effects are important. Finally, the small flaw problem, wherein crack growth rate is apparently accelerated relative to the large flaw problem, cannot be currently explained by elastic fracture mechanics considerations.

The development of improved models for the crack growth problem for the full range of these problems is crucial to the damage tolerance assessment needs for advanced aerospeace structures. The overall objective for the current research is to provide an improved basis for making damage tolerance assessments through numerical modeling of crack tip behavior, including the effects of plastic or other residual strains. The elastoplastic BIE method is the basis for the current effort.

The first goal of the originally proposed program is to extend an existing planar elastic fracture mechanics analysis based on the BIE methodology to the analysis of plastic zones around cracks. The second proposed goal is to establish fundamental results for crack tip elastoplastic behavior, based on a numerical and analytical study of the elastoplastic BIE formulation. The third proposed goal is to establish the credibility of the elastoplastic BIE formulation relative to the finite element method for refined numerical analysis of the nonlinear fracture mechanics problem, and to apply the capability to important problems of fatigue crack growth modeling for advanced aerospace structures. The goal for the second year of the effort is to extend the research to the problem of modeling crack extension under elastoplastic conditions.

The specific objectives for the research effort as stated in the proposal are as follows. Through basic research in the elastoplastic BIE method, establish:

1. Cost effective and highly accurate computational method for planar fracture mechanics models including inelastic effects near the crack tip.

2. Direct comparisons between the inelastic BIE fracture mechanics code and an advanced finite element code.

3. Advanced computational procedure for investigating history dependent fatigue crack growth processes.

4. Feasibility of the direct numerical analysis of elastic and inelastic response to growing cracks; the results of this capability can shed light on the plastic wake phenomena for growing fatigue cracks.

All first year goals and objectives have been met. New understanding of the problems associated with modeling crack growth problems has been achieved. The next section summarizes these findings.

RESEARCH STATUS

Review of the Mathematics

A complete treatment of the elastic formulation for the Green's function BIE model for cracked planar problems is given by Snyder and Cruse [1] and Cruse [2]. The full development of the elastoplastic solution is given by Cruse and Polch [3]. The following summarizes these developments:

The basic BIE formulation for a crack problem, as illustrated in Figure 1. is given as follows

$$C_{ji}u_i(P) + \int_S T^*_{ji}(P,Q)u_i(Q)ds + \int_\Gamma T^*_{ji}(P,Q)u_i(Q)ds = \int_S U^*_{ji}(P,Q)t_i(Q)ds + \int_\Gamma U^*_{ji}(P,Q)t_i(Q)ds \qquad (1)$$

In (1) the u_i, t_i terms are the boundary displacement and traction vectors for the modeled problem. The kernel functions (or influence functions) U_{ij}^*, T_{ij}^*, are mathematical entities giving the displacement and traction that are computed on S, Γ for the problem of an infinite body loaded at $p(\mathbf{x})$, $P(\mathbf{x})$[†] by a set of unit point loads in each coordinate direction. The star on the kernel functions denotes the addition to the point load solution of the terms necessary to provide for a traction free crack at a specified location and orientation in the geometry.

The use of a Green's function for special geometries is well developed in potential theory, as discussed by Greenberg [4]. In the current application we seek to obtain fracture mechanics solutions for the case of traction free cracks in finite planar bodies. The term with $t_i(Q)$ for $Q\varepsilon\Gamma$ in (1) is therefore zero, as shown. The use of the cracked body Green's function results in the traction kernel also being zero on the crack, viz. $T_{ij}^*(P,Q) \equiv 0, Q \varepsilon \Gamma$, also as shown in (1).

Thus (1) constitutes the constraint equation that must be satisfied by u_i, t_i on the uncracked portion of the surface. This equation can be reduced to solvable, algebraic form through the use of suitable approximations to the

[†]Lower case $p(\mathbf{x})$ is an interior point; upper case $P(\mathbf{x})$ is a boundary point.

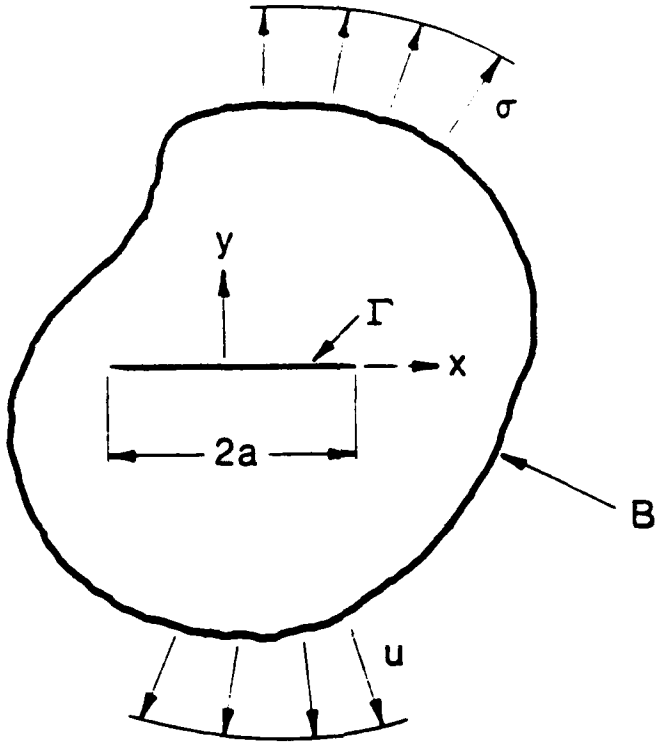

Figure 1. Basic Geometry for Green's Function Formulation

boundary data u_i, t_i. In the current application we use the approximation of piecewise linear interpolations of u_i, t_i as developed by Cruse [2].

The form of (1) for the interior displacement provides a means of direct computation of interior strains, stresses, and stress intensity factors. Simply stated, the interior quantities depend on the totality of boundary data for u_i, t_i through integration of these quantities together with appropriate kernel functions for the cracked plane.

Introduction of anelastic strains (e.g., residual strains due to welding, thermal gradient strains, elastoplastic strains) $\varepsilon_{i\ell A}$ to the BIE formulation [††] results in a modification to (1)

$$C_{ji}\dot{u}_i(P) + \int_S T_{ji}^*(P,Q)\dot{u}_i(Q)ds = \int_S U_{ji}^*(P,Q)\dot{t}_i(Q)ds + \int_{<A>} \Sigma_{ji\ell}^*(P,q)\dot{\varepsilon}_{i\ell}^A(q)dA \qquad (2)$$

The addition of the volumetric (area in 2D) integral in (2) is seen as a correction term to the elastic BIE, (1). The kernel function $\Sigma_{ji\ell}^*$ in this new integral consists of derivatives of the elastic displacement kernel U_{ij}^*, and its form differs for plane stress or plane strain.[5]

Equation (2) no longer provides a direct means for computing the boundary data, except when $\varepsilon_{ij}^A(q)$ is specified. Thus, for elastoplastic response, an additional relationship is needed to compute the plastic strains for (2). The appropriate equation is the interior strain distribution, as written by Cruse and Polch [3].

$$\dot{\varepsilon}_{ij}(p) = \int_S S_{kij}^*(p,Q)t_k(Q)ds + \int_S D_{kij}^*(p,Q)u_k(Q)ds + \int_{<A>} (\Sigma_{i\ell m,j}^* + \Sigma_{j\ell m,i}^*)\dot{\varepsilon}_{\ell m}^A(q)dA + E_{i\ell mj}\dot{\varepsilon}_{\ell m}^A(p) \qquad (3)$$

This equation (3) computes the interior <u>total</u> strain in terms of the boundary data and the interior anelastic strains. For elastoplastic solutions, the unknown data $\dot{u}_j$, $\dot{t}_i$, $\dot{\varepsilon}_{ij}^A$ are solved for incrementally and equations (2), (3) are coupled on an iterative basis. The interior anelastic strains are modeled as piecewise constant over ΔA_i area segments in the current study. The full solution algorithm for the elastoplastic case is given in Figure 2. The yield criterion has to be satisfied, giving the amount of total strain that is plastic at each load level. The use of iteration as opposed to

---

[††]The dots on the variables denote an increment in the variable.

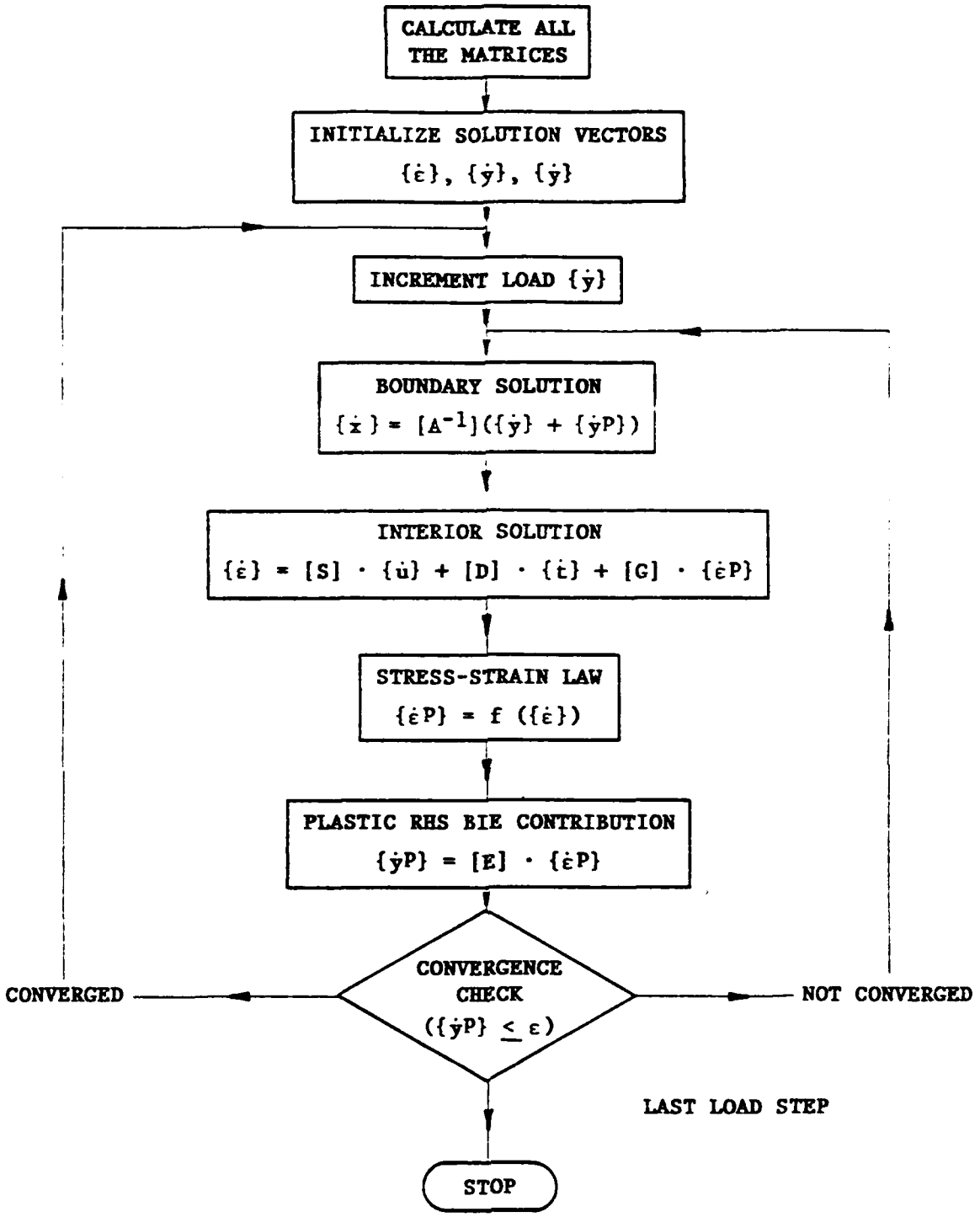

Figure 2. Elastoplastic Solution Algorithm

a tangent modulus formulation allows us to precompute all of the elastic kernel functions, to invert one of these, and to perform all of the ensuing numerics as matrix multiplications.

Stress Intensity Factor Computations

The structure of (3) has been investigated by Cruse and Polch [3] for interior points approaching the crack tip. It was found that, for the elastoplastic case where the crack tip strains can exhibit a singularity up to $1/\rho$ (where ρ is the distance from the crack tip), eq. (3) still results in convergent integrals in (2), (3). However, the actual strength of the plastic strain singularity is a function of the work hardening (see Hutchinson [6]) and can only be inferred from the resulting strain distributions after satisfying the yield criterion implicit in (3).

The elastic stress intensity factor computation for the BIE formulation using the cracked Green's function results directly from the elastic version of (3). As shown by Snyder and Cruse [1], the kernels in the two boundary integrals in (3) are explicitly dependent on the inverse-square root of the distance of $p(\mathbf{x})$ from the crack tips (+/-a). Further, for the nonsingular distribution of anelastic strains in (3), the volumetric kernel has the same explicit dependence. Thus, for nonsingular, anelastic strains we obtain the following direct, path independent evaluation of the elastic stress intensity factors

$$(K_I, K_{II}) = -\int_{S_R} {}^{I,II}(Q)u_i(Q)ds + \int_{S_L} {}^{I,II}(Q)t_i(Q)ds + \int_A M_{ij}{}^{I,II}(q)\varepsilon_{ij}{}^{A}(q)dA \qquad (4)$$

The first two terms in (4) are those previously used by Snyder and Cruse [1] and by Stern, et al. [7]. These are path independent integrals which provide a simple quadrature for computing K_I, K_{II} from any solution for u_i, t_i on a path around the crack, but excluding the crack.

Equation (4) states that nonsingular, anelastic strains modify the elastic K_I, K_{II} values in an equally simple sense of quadrature when these quantities are specified in the volume (area). Some examples of this quadrature for a notch plasticity problem will be discussed below.

In developing eq. (4), it was assumed that the anelastic strains were nonsingular, thus neglecting the crack tip elastoplastic effects. The additional terms, reflecting the higher order singular behavior, are represented by the incremental elastoplastic strain portion of eq. (3)

$$\dot{\varepsilon}_{ij}^{P}(p) = \int_{<A>} (\Sigma_{i\ell m,j}^{*} + \Sigma_{j\ell m}^{*})\, \dot{\varepsilon}_{\ell m}^{P}(q)\,dA + E_{i\ell mj}\, \dot{\varepsilon}_{\ell m}^{P}(p) \qquad (5)$$

As discussed by Cruse and Polch [3], eq. (5) is dimensionally homogeneous for any, physical singularity in plastic strain increment as $p(\mathbf{x})+/-a$, but the order of the singularity is not directly solvable from (5).

A considerable number of technologically important problems to the aerospace industry are associated with the use of linear elastic fracture mechanics parameters (i.e., K_I, K_{II}) for problems of limited or localized plasticity. These include predicting K_I for cracks which are undergoing cyclic plasticity resulting in crack closure effects on spectrum crack growth, and cracks growing ir the plastic zone of a bolthole subject to high loading or prestressing.

The present research seeks to shed light on some of these problems by presenting a stress intensity factor computation algorithm that can directly and unambiguously model these kinds of limited plasticity effects. For such problems, the solution given in (4) is to be used. The two boundary data integrals in (4) reflect the plastic strain distribution of the crack tip, as well as other inelastic strains through the volume integral in (2). Secondly, the prior plasticity of a notch will affect K_I, K_{II} through the volume integral of those nonsingular strains in (4). The resulting values of K_I, K_{II} are the plasticity corrected elastic stress intensity factors which define the strength of the elastic singularity which dominates the plastic singularity. The use of this approach is obviously limited to crack tip plastic zones which are contained within the field of the elastic singularity.

Numerical Solution Algorithm

Application of the appropriate interpolations to the data in eqs. (2) and (3) reduces the integrals to algebraic form. In general, the boundary solution involves an equal number of known (applied) boundary data and unknown data. Letting the unknown data be given by $\{\dot{x}\}$, the product of the known data and its coefficient matrix terms by $\{\dot{y}\}$, and the coefficient of the piecewise constant plastic strains by [E], we obtain from (2)

$$[A]\{\dot{x}\} = \{\dot{y}\} + [E]\{\dot{\varepsilon}^{P}\} \qquad (6)$$

Similarly, taking [S] and [D] to be the elastic coefficient arrays of the boundary data, and [G] to be the elastic coefficient array for the plastic strain, then eq. (3) becomes

$$\{\dot{\varepsilon}^{T}\} = [S]\{\dot{t}\} + [D]\{\dot{u}\} + [G]\{\dot{\varepsilon}^{P}\} \qquad (7)$$

The strain superscripts in (6) and (7) refer to total (elastic plus plastic) and plastic values, while the dots imply that all of the variables are to be interpreted in terms of their incremental evaluation.

The present BEM algorithm makes use of the Huber-Mises-Hencky yield condition and associated flow rule. Elastic, perfectly plastic material response was modeled throughout this study, but the code allows for a multi-piecewise-linear definition of a general stress-strain curve.

Following the approach adopted in the ADINA code, each increment in total strain is divided into subincrements (Bathe [8]). The number of subincrements is selected to minimize the error in the deviatoric stress change within the strain increment. The stress increment for a given iterate of increment in plastic strain is then obtained by an Euler forward integration of the flow rule, according to

$$\{\sigma_{\substack{\text{CURRENT}\\\text{LOAD}}}\} = \{\sigma_{\substack{\text{PREV}\\\text{LOAD}}}\} + \int_{\substack{T\\\text{PREV}\\\text{LOAD}}}^{\substack{T\\\text{CURRENT}\\\text{LOAD}}} [C^{EP}]d^{T} \qquad (8)$$

In eq. (8), the elastoplastic matrix relating the subincrements in stress and total strain is given for plane strain by

$$d\sigma_{ij} = 2G[\delta_{im}\delta_{jn} + \frac{\nu}{1-2\nu}\delta_{mn}\delta_{ij} - \frac{S_{ij}S_{mn}}{2J_2(1+H/3G)}]d\varepsilon^{T}_{mn} \qquad (9)$$

The current state of deviatoric stress, S_{ij}, and second invariant of deviatoric stress, J_2, is updated within the subincremental integration of (8). The tangent modulus, H, is taken as the slope of the effective stress-effective plastic strain curve, at the current level of effective stress.

Figure 2 summarizes the current iteration algorithm for the solution of eqs. (6,7). The coefficient arrays [A], [S], and [D] depend solely on the elastic constants of the material and the boundary shape. Thus, they are computed once and stored. The [A] matrix is inverted prior to storage. The interior arrays [E] and [G] are also dependent solely on the elastic constants and the interior element modeling. These are also computed once and stored. Note again that only that portion of the interior expected to be inelastic need be modeled. The expense of generating [E] and [G] for crack problems dictates that such limited volumetric modeling be employed.

In the first iteration at a given load step, the plastic strain increment in Figure 2 is taken from the last load step. The boundary solution then responds, in an elastic manner, to the increase in loading. Estimated interior total strains are then calculated. Based on the new total strain increment, the interior stresses and plastic strains are computed based on satisfying the yield condition through eq. (8). The plastic strain increment is then updated in both eqs. (6,7) for a recalculation of the boundary and interior solutions.

Absolute convergence of the strain solution within each element is required for the iteration process used. That is, the maximum difference

between successive iterates of the plastic strain correction term (second term on the right hand side of eq. (6)) is not allowed to exceed a user-specified tolerance. This tolerance has been selected on the basis of its ability to relate directly to the amount of the displacement increment. A number of numerical experiments with tolerances ranging over 10^{-6} to 10^{-9} were conducted to test the sensitivity of the results to this value. It was found that the errors in the displacements, for a simple uniform stress test case, were of the order of the tolerances specified. A decrease in the tolerance by an order of magnitude generally resulted in a doubling of the number of iterations required to achieve convergence. A value of 10^{-7} was used for the notch problem and a value of 10^{-9} was used for the fracture mechanics problem, in order to account for the higher strain gradient.

Numerical Results

The computer program has been verified on two example problems. The first is a plate with perforations, previously solved by Haward and Owen [9] using finite elements and resolved by Telles [10] using the BEM. This example served the basic purpose of validating the current code and provided a basis for some numerical experimentation. The second problem is a fracture mechanics problem of a center cracked plate loaded in tension. The plastic strain results are compared to ADINA results using a singular finite element model.

The geometry for the first problem is shown in Figure 3. Plane strain conditions are applied for all three of the analyses and the material is taken to be elastic-perfectly plastic. The appropriate constants are $E = 42. \times 10^3 MN/m_2$, $\sigma_y = 105.\ MN/m^2$, $\nu = 0.33$. The one loading condition considered was uniaxial tension, applied by prescribing displacements at the edges of the plate section. The piecewise linear plastic strain BEM mesh of Telles is shown in Figure 3; the FEM quadratic isoparametric element mesh used by Haward and Owen is shown in Figure 4. The current BEM mesh, using piecewise constant plastic strains, is shown in Figure 5.

Figure 6 plots the numerical results in terms of the amount of force required versus the applied displacements. Table 1 summarizes the numerical force-displacement data. All three model results show excellent agreement, given the disparity in modeling strategies. The predicted limit load for the current study differs from the other two by less than 2%. The difference is attributed to the use of constant strain elements. Limit load is obtained when the centroidal value of stress in the last ligament element yields, a condition that will occur below the load for yielding the last physical ligament ahead of the notch.

The current BEM code was tested for a range of load increments in a deliberate attempt to create numerical instability. The numerical results plotted in Figure 7 were generated using an incrementation scheme resulting in a single element yielding at a time. The BEM results required about twenty iterations per load step to fully converge. The worst case was one load step to the maximum displacement. The solution converged in 45 iterations and agreed with the other limit load results within 0.2%. The maximum deviation in calculated plastic strains was 10% in the last element to yield.

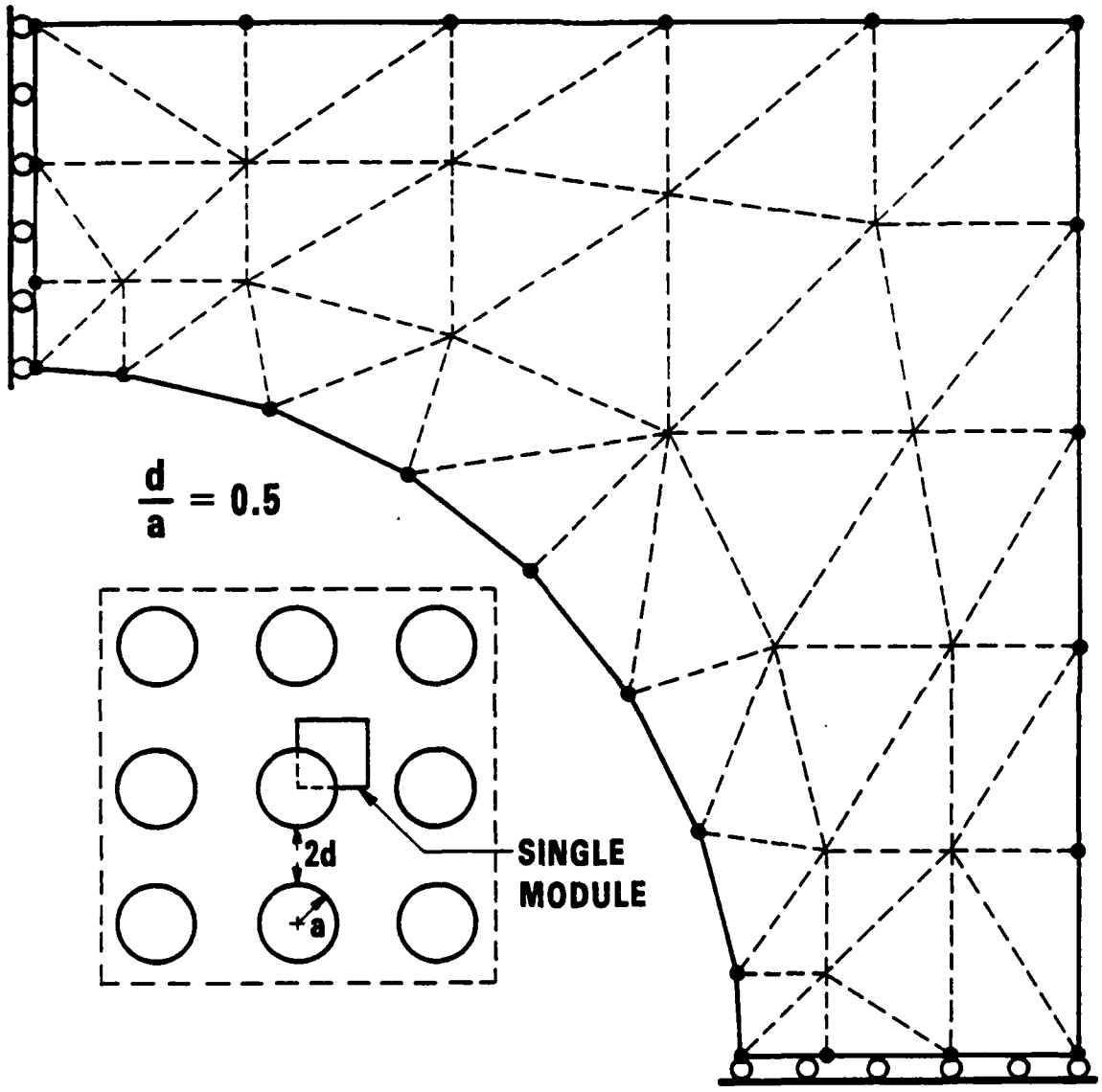

Figure 3. Perforated Polystyrene Plate and BIE Discretization Used by Telles (1983)

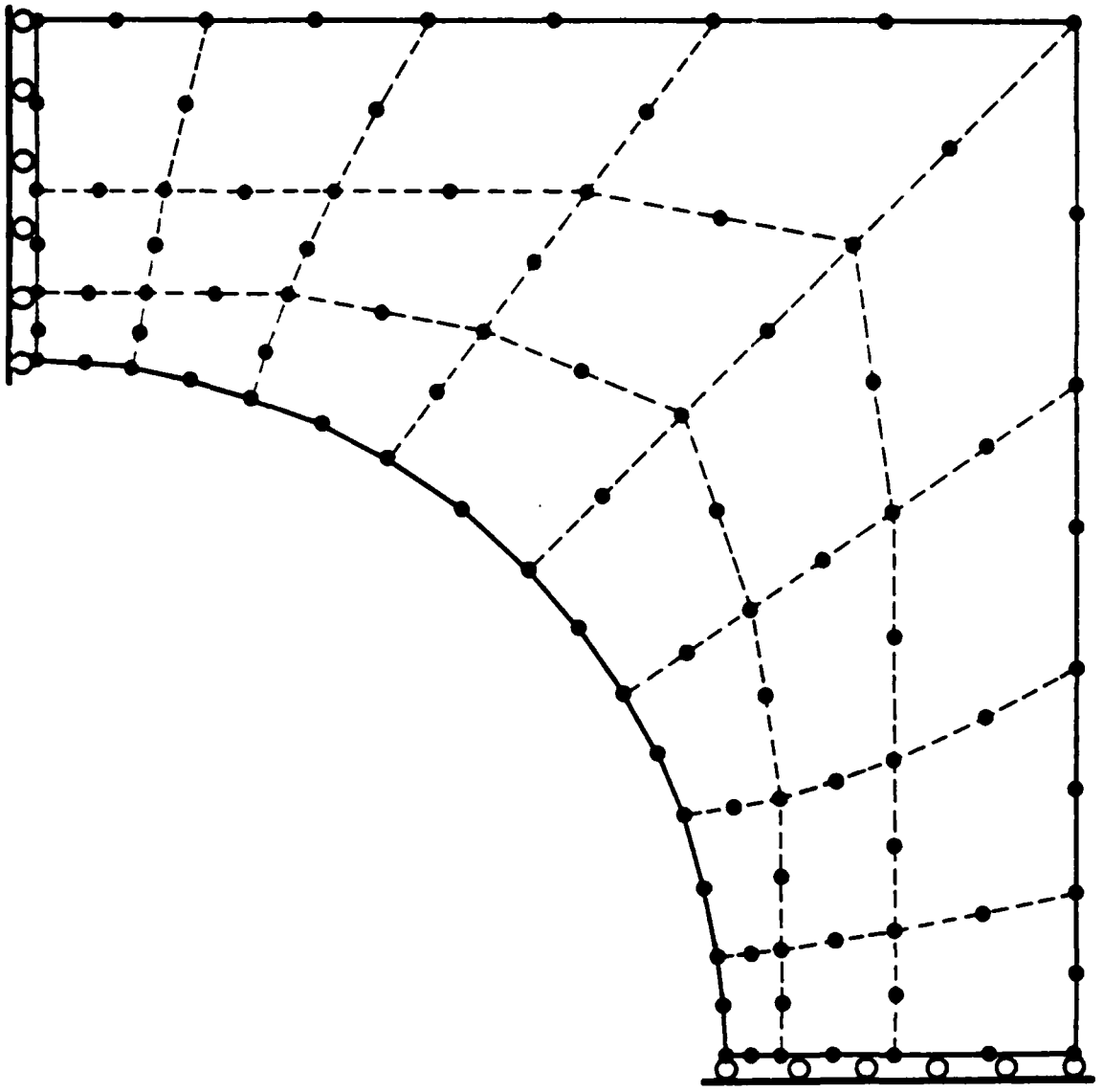

Figure 4. Quadratic Isoparametric Finite Element Mesh
Used by Haward and Owen (1973)

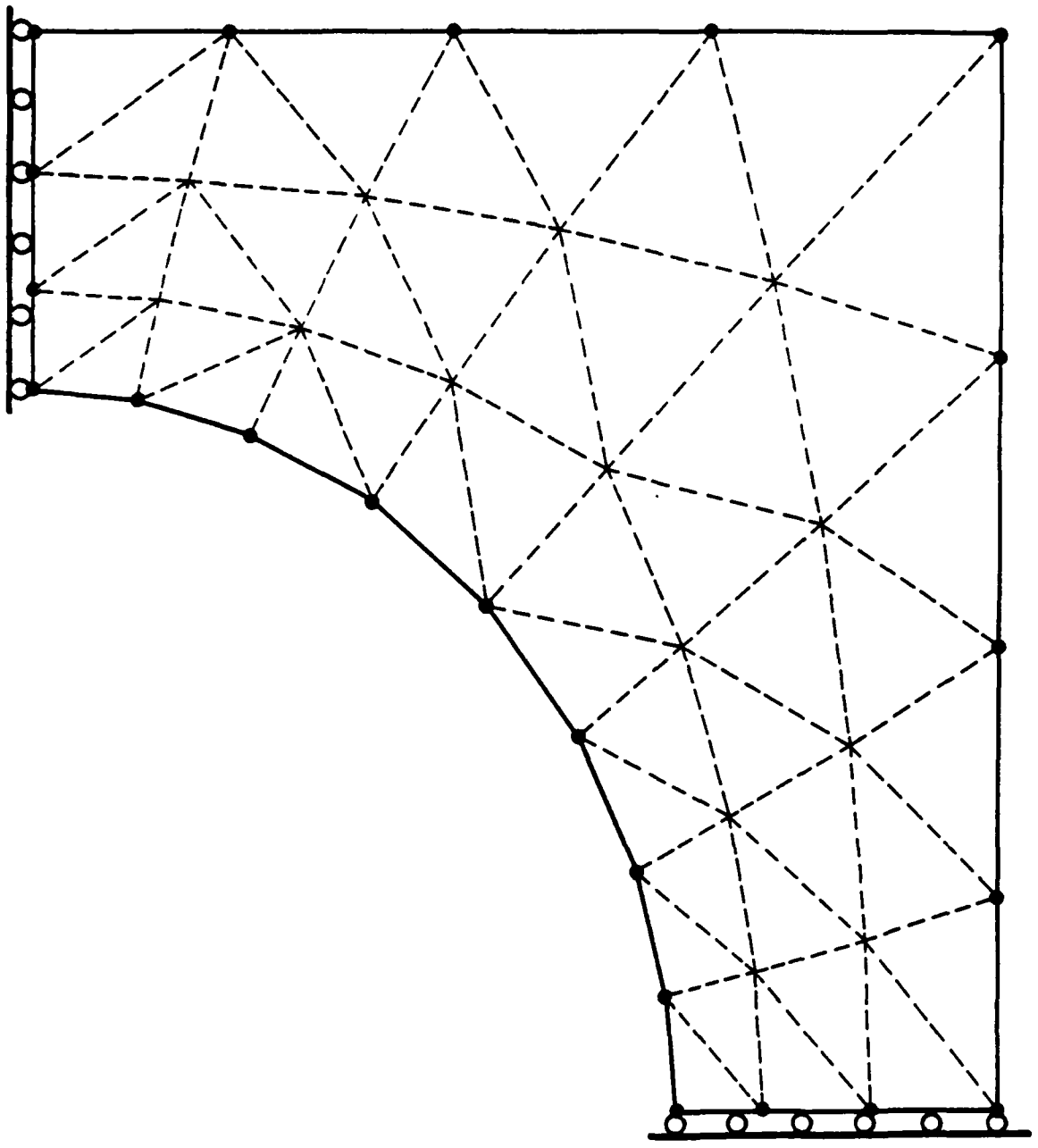

Figure 5. BIE Discretization Used in the Present Study

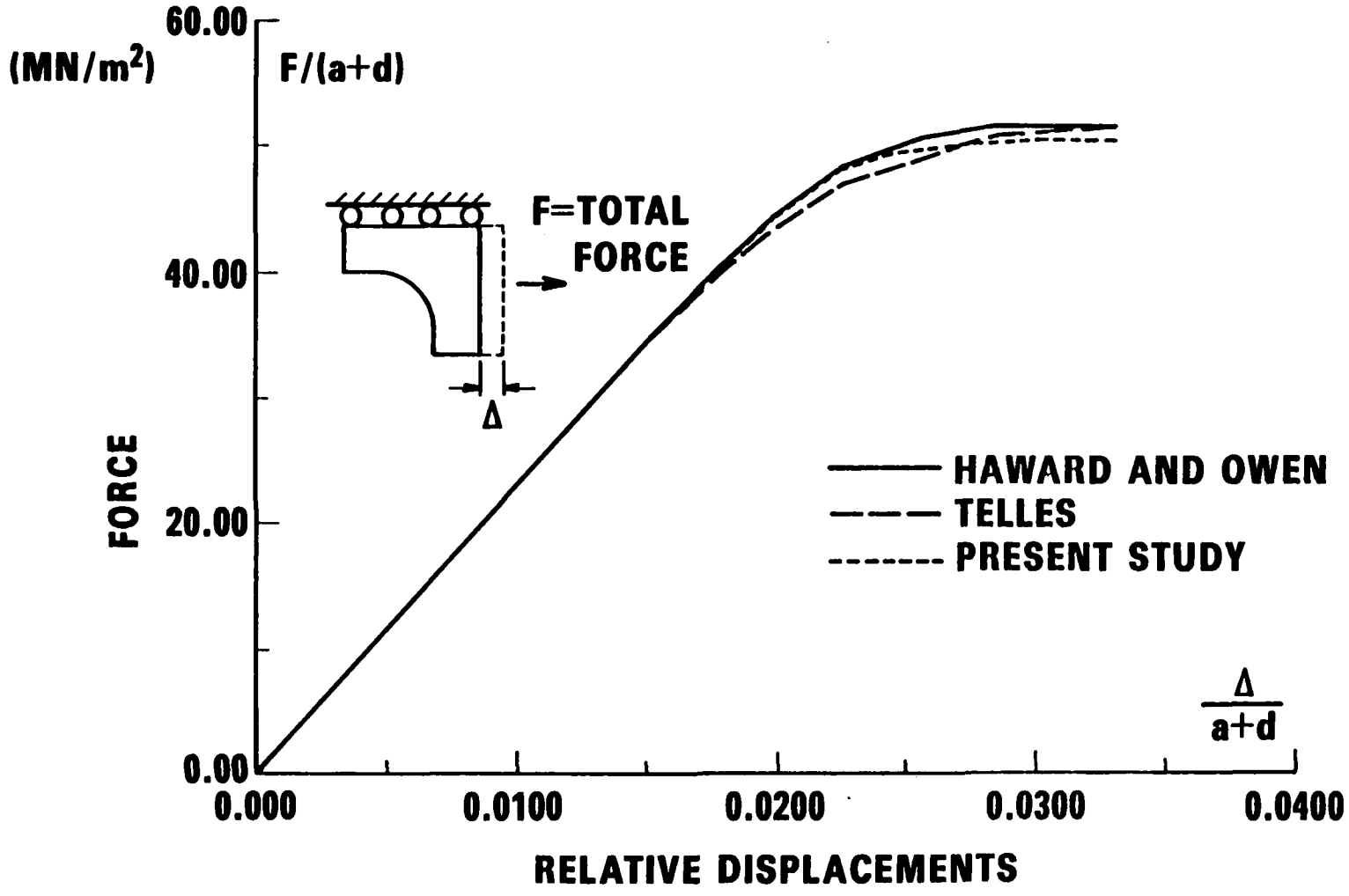

Figure 6. Results of the Polystyrene Plate Problem

Table 1.

Numerical Results of the Polystyrene Plate Problem

PCP - Uniaxial Stretch

Load Case	Load %	Displacement (A $\times 10^{-3}$	Force (F)	$\frac{\Delta}{a+d}$ (x 10-z) [%]	F/(a+d)
1	.50	4.5	10.3576	1.50	34.525
2	.55	4.95	11.3259	1.65	37.753
3	.60	5.4	12.2459	1.80	40.820
4	.65	5.85	13.1047	1.951	43.682
5	.70	6.3	13.8412	2.10	46.137
6	.75	6.75	14.4610	2.25	48.203
7	.80	7.2	14.7765	2.40	49.255
8	.85	7.65	14.9091	2.55	49.697
9	.80	8.1	15.0009	2.70	50.003
10	.95	8.55	15.0650	2.85	50.217
11	1.00	9.0	15.1112	3.00	50.371
12	1.05	9.45	15.1412	3.15	50.471
13	1.10	9.9	15.1412	3.30	50.471

The ultimate strength = 50.471 MN/m^2

a, d defined in Figure 2

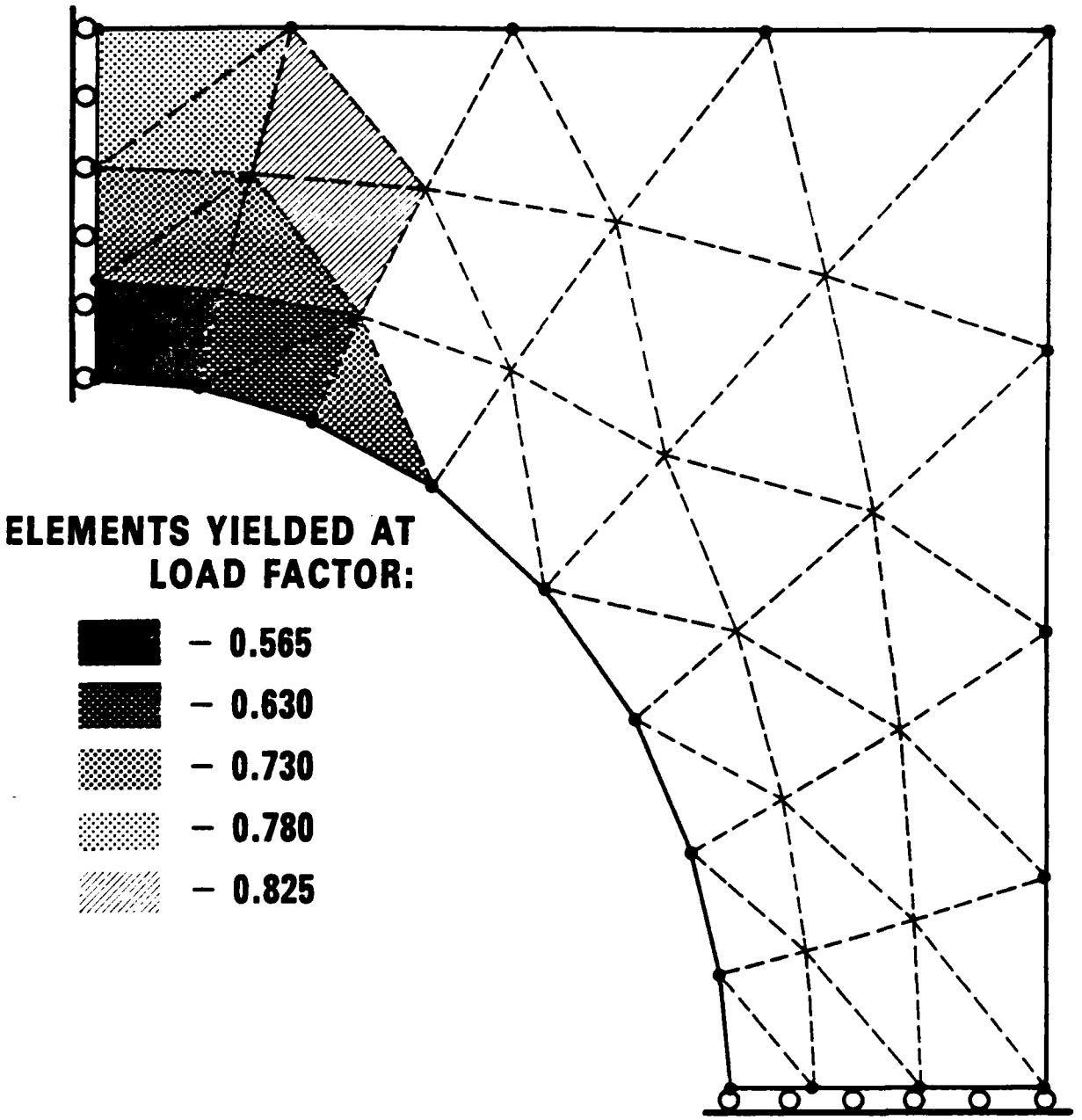

Figure 7. Growth of the Plastic Zone

The second example is a center-cracked plate loaded in tension. The total width of the plate is 8 units, with a crack size of 2 units. One quarter of the geometry was modeled using ADINA, as shown in Figures 8 and 9. Extremely fine resolution of the crack tip elements was taken in order to minimize the error in the finite element solution. The elastic stress intensity factor for this finite element model, using the crack opening displacement at the quarter-point node, was in error relative to handbook values by about 2%.

The BEM mesh corresponding to the local finite element scale is shown in Figure 10. The elastic BEM stress intensity factor results were indistinguishable from the handbook results. The FEM/BEM meshes were selected so as to provide about three decades of plotting data in terms of crack tip distance. The maximum size of the plastic zone was limited solely for convenience in the current study.

Plane strain conditions were used for both of the models. The elastoplastic material constant used were $E=2.037\cdot10^5 MN/m^2$, $\sigma_y=3.452\cdot10^2 MN/m^2$, and $\nu=0.27$.

The ADINA crack tip model used quadratic, isoparametric finite elements with nine interior strain integration points. The BEM model used constant strain triangles throughout. As noted above, both meshes were identical in the crack tip region. The ADINA model used one layer of collapsed quadratic elements adjacent to the crack tip. This approach induces a (1/r) type of singularity in the displacement gradient within this first layer of elements. No singularity modeling is used in the BEM plastic strain distribution.

Loading history was identical for both models and spans the range of load factors of 0.0310 to 0.2075. A value of 1.0 corresponds to yielding of the whole plate. A total of 68 load steps was used for both models. The load steps satisfy the conditions of Larsson and Carlsson [11]. Simply stated, these conditions require that at most one element becomes plastic at each load increment, and that the load increment should be smaller than 1% of the load corresponding to $K_{Imax}=\sigma_y\cdot\sqrt{a}$. The range of load factors has been chosen as the range to go from yielding the innermost element to yielding the outermost element.

ADINA failed to converge for the first step until the stiffness reformulation (BFGS) procedure was used. After the first load step (requiring 20 iterations) the ADINA algorithm with reformulation generally converged with five iterations. The BEM algorithm, using elastic "stiffnesses," converged in ten to fifty increments at each load step with the higher numbers occurring at the higher load levels. The total computer time for the two models was essentially the same, although the BEM calculations are cheaper per load step. A higher final load level or cyclic loading would yield a benefit to the BEM model, even though the current BEM code is not yet optimized for these calculations.

The crack tip plastic strain distribution results are shown in Figure 11 for two of the computed load levels. The data are taken from points distributed near, but not on, a line at an angle of about 85° to the plane of the crack. This angle corresponds to the line of maximum equivalent elastic

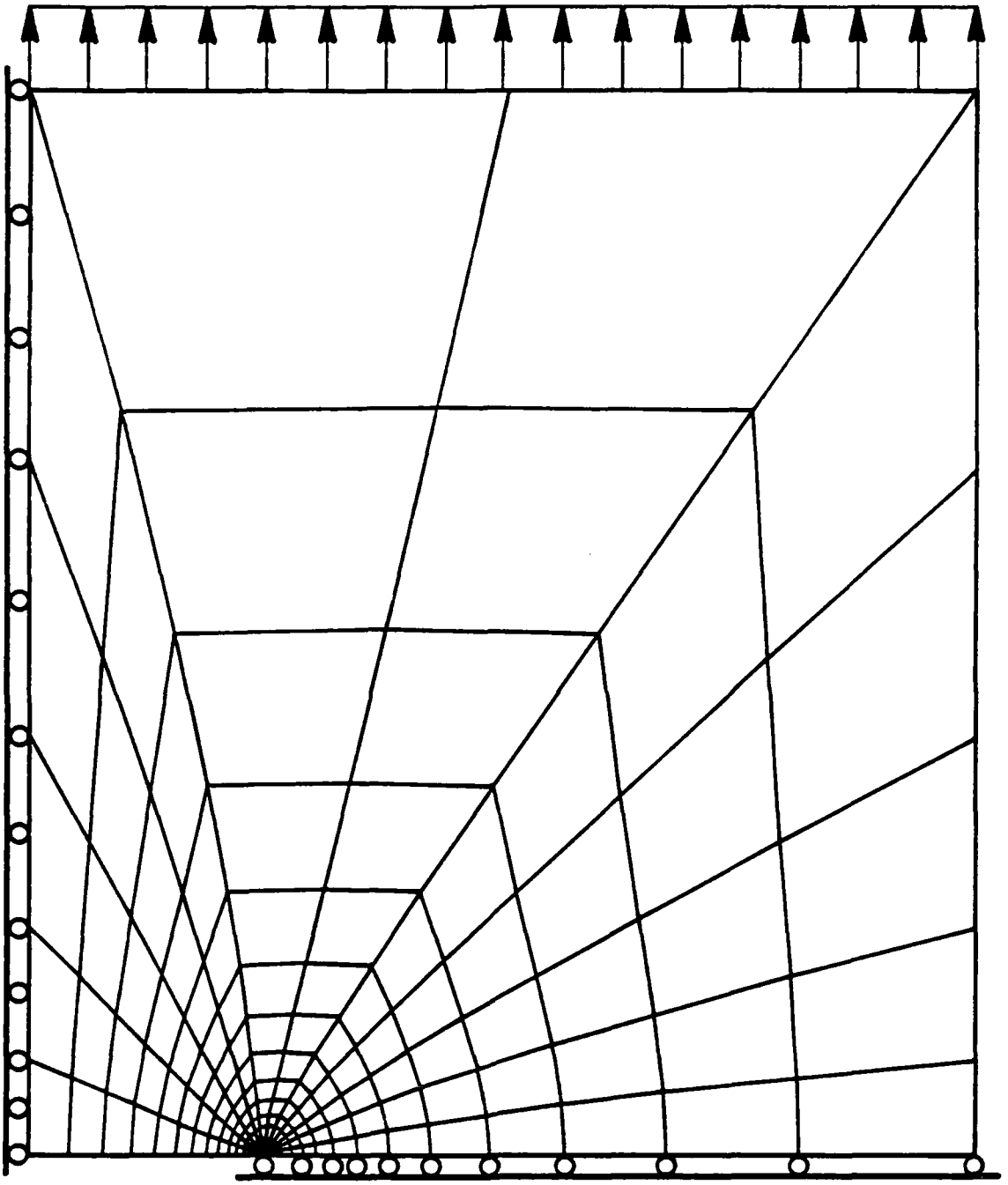

Figure 8. Finite Element Mesh of the Center-Cracked Plate

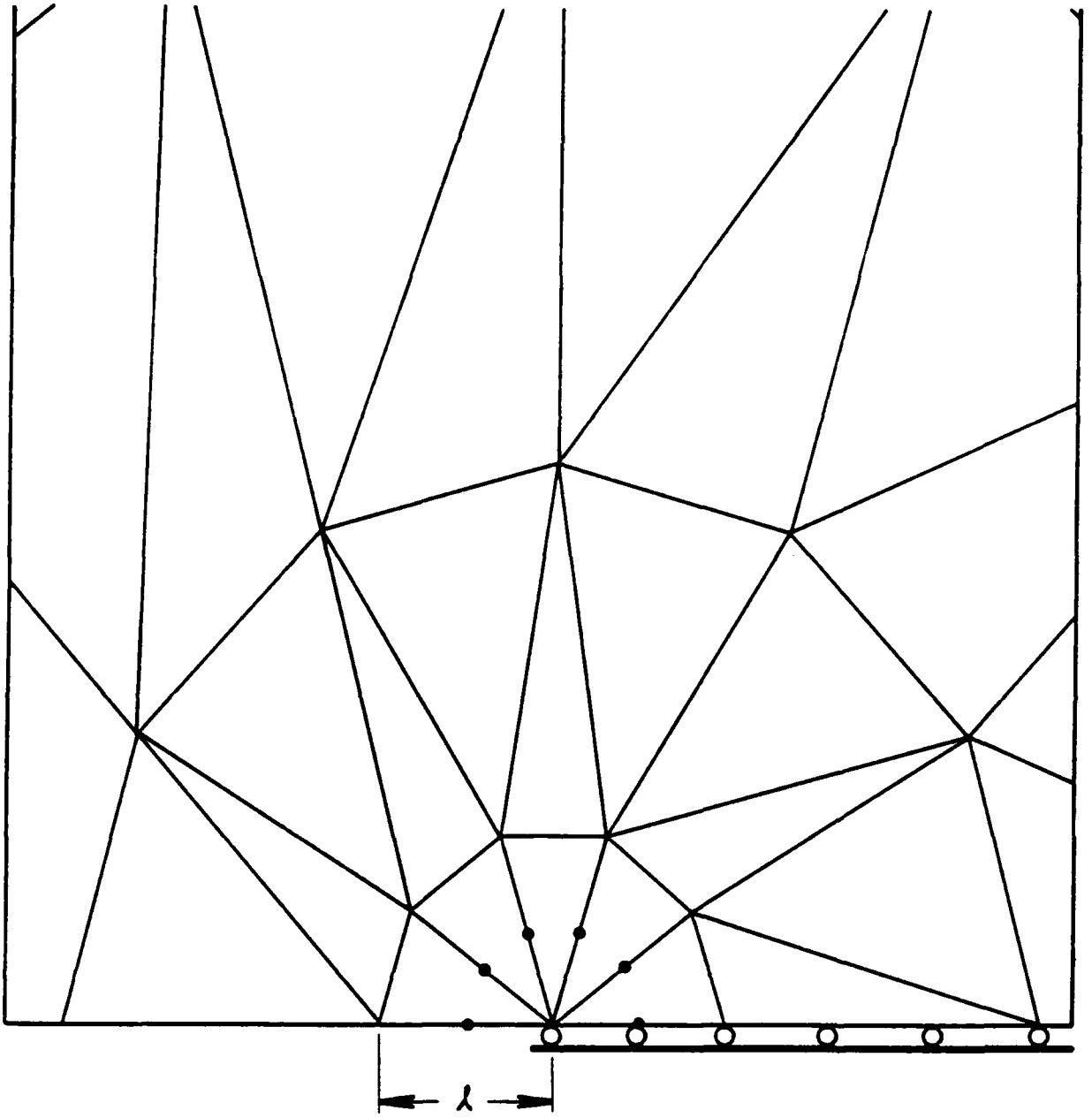

Figure 9. Finite Element Modeling of the Crack Tip Vicinity with Singular Elements ($\ell/a = 0.001$)

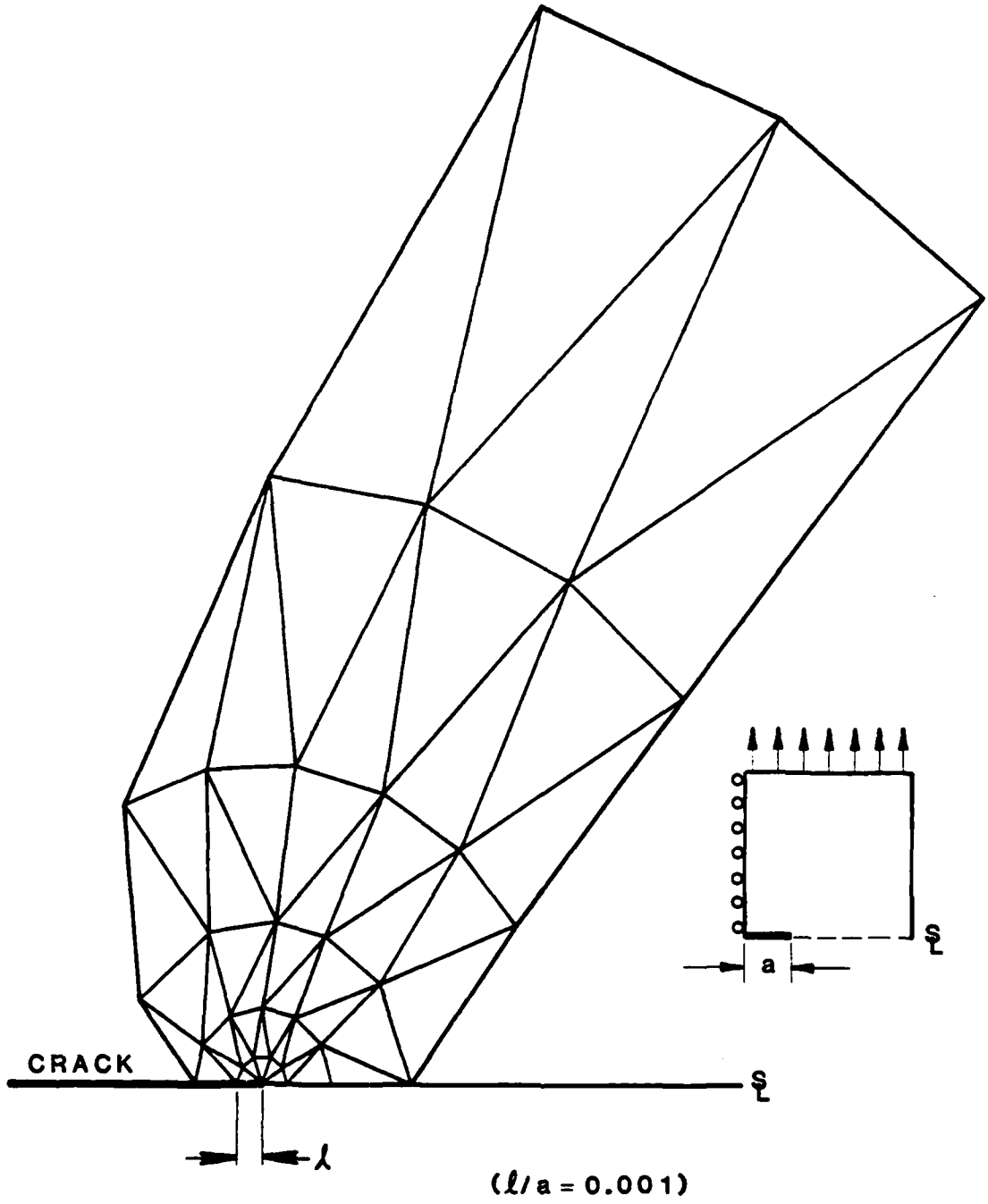

Figure 10. Internal Plastic Strain Elements for the Boundary Integral Equation Modeling of the Crack Tip Vicinity ($\ell/a = 0.001$)

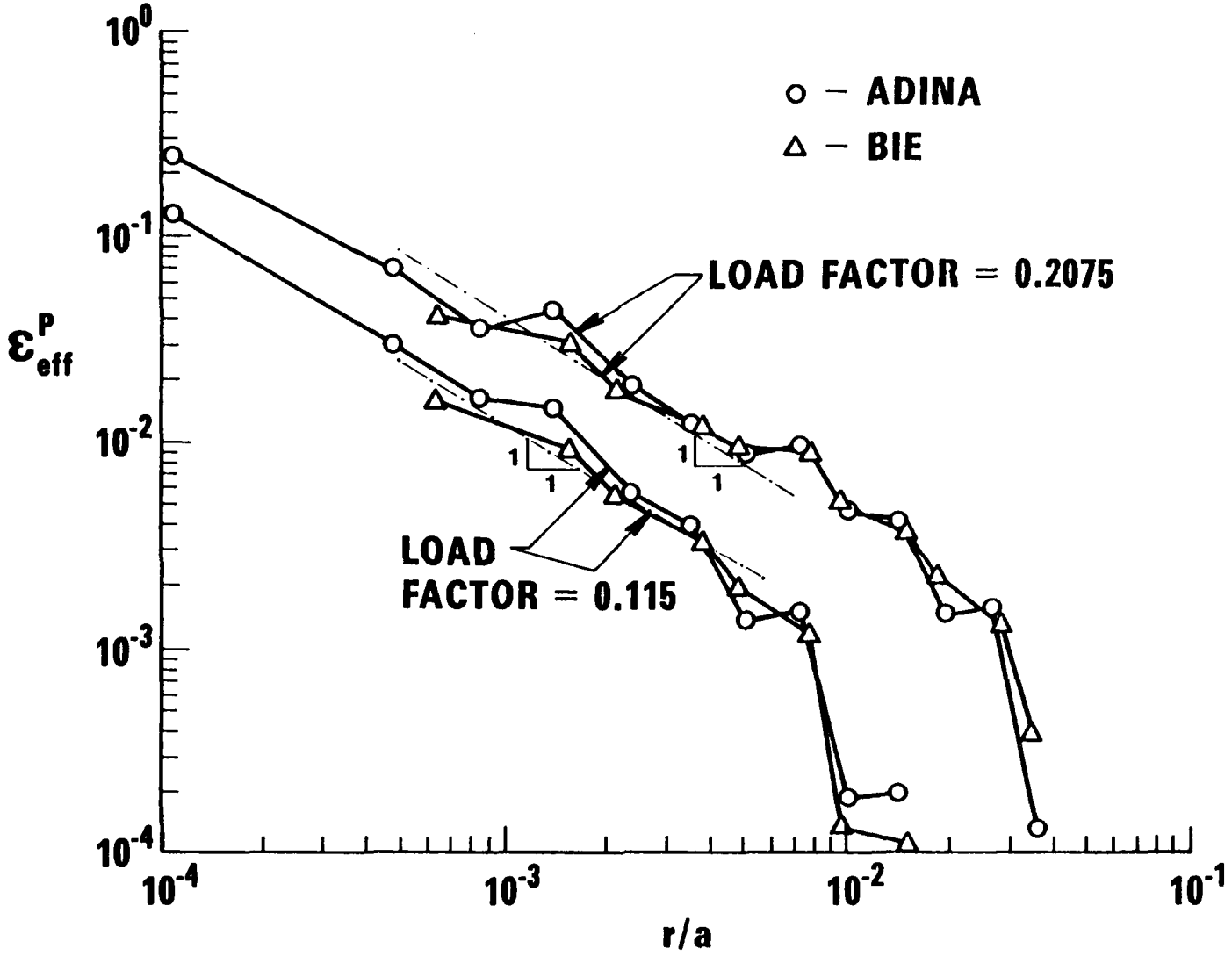

Figure 11. Effective Accumulated Plastic Strain Distribution

strain. The jaggedness of the curves is mostly due to the use of triangular elements, as well as to the points having different angular locations. The data is plotted in terms of the centroidal value of plastic strain. The innermost row of finite elements has three sampling points radially, which accounts for the smaller radius plotted for these results. The numerical results from ADINA show a tendency for a spurious peak in plastic strain increments in the second row of elements. This peak is no doubt induced by the lack of a singularity-transition element in the current study.

It is significant to find that the numerical results are in such good agreement. This confirms the accuracy of the BEM algorithm for piecewise constant plastic strains. The BEM results do not show the strength of the plastic singularity as strongly in the first row of elements as do the finite element results, with the imbedded 1/r singularity in displacement gradient. However, both sets of results strongly indicate that the plastic strain for localized plasticity possesses the same 1/r singularity that is associated with fully developed plasticity for the case of zero strain hardening. Clearly, the presence of the underlying elastic singularity field plays an important role in enhancing the modeling accuracy for crack tip plasticity.

Figures 12 and 13 show the progressive development of the plastic zone up to the maximum modeled load. It is to be emphasized that the current study was intended to confirm the accuracy of the new BEM algorithm for elastoplastic fracture mechanics analysis, and not study extensive plasticity response at the crack tip. For this reason the current results were not carried beyond the load level shown. There is no inherent limit to the load level that can be modeled with this BEM algorithm.

The next problem was selected to validate the stress intensity factor algorithm for prior plasticity for any residual or thermal strain field. The geometry selected is a simple tension specimen with the boundary and internal mesh shown in Figure 14. The mesh arrangement was selected solely for convenience, as it is used as a portion of a later mesh. The specimen was loaded to 110% of the yield stress for a bilinear material response. This induced a uniform plastic strain throughout the specimen.

The next step in the validation of eq. (4) was to introduce a crack, done along the bottom of the mesh as shown. The residual boundary solution corresponding to the residual internal strains is computed for the cracked case by eq. (6). Next, the internal strains for the residual boundary and internal variables are computed from eq. (7). In the case of the test problem, eq. (6) produced the uniform displacements compatible with uniform residual strains, eq. (7) computed internal strains equal to the residual strains.

The elastic stress intensity factor for the problem was then computed for the residual boundary terms computed from (6). If there were further changes in the residual strains due to unloading plasticity, these would modify the elastic strain intensity factor through the appropriate term in eq. (4). As required for this simple case, the residual stress intensity factor was zero. The residual values in the first and third terms in eq. (4) cancel each other to within computer accuracy.

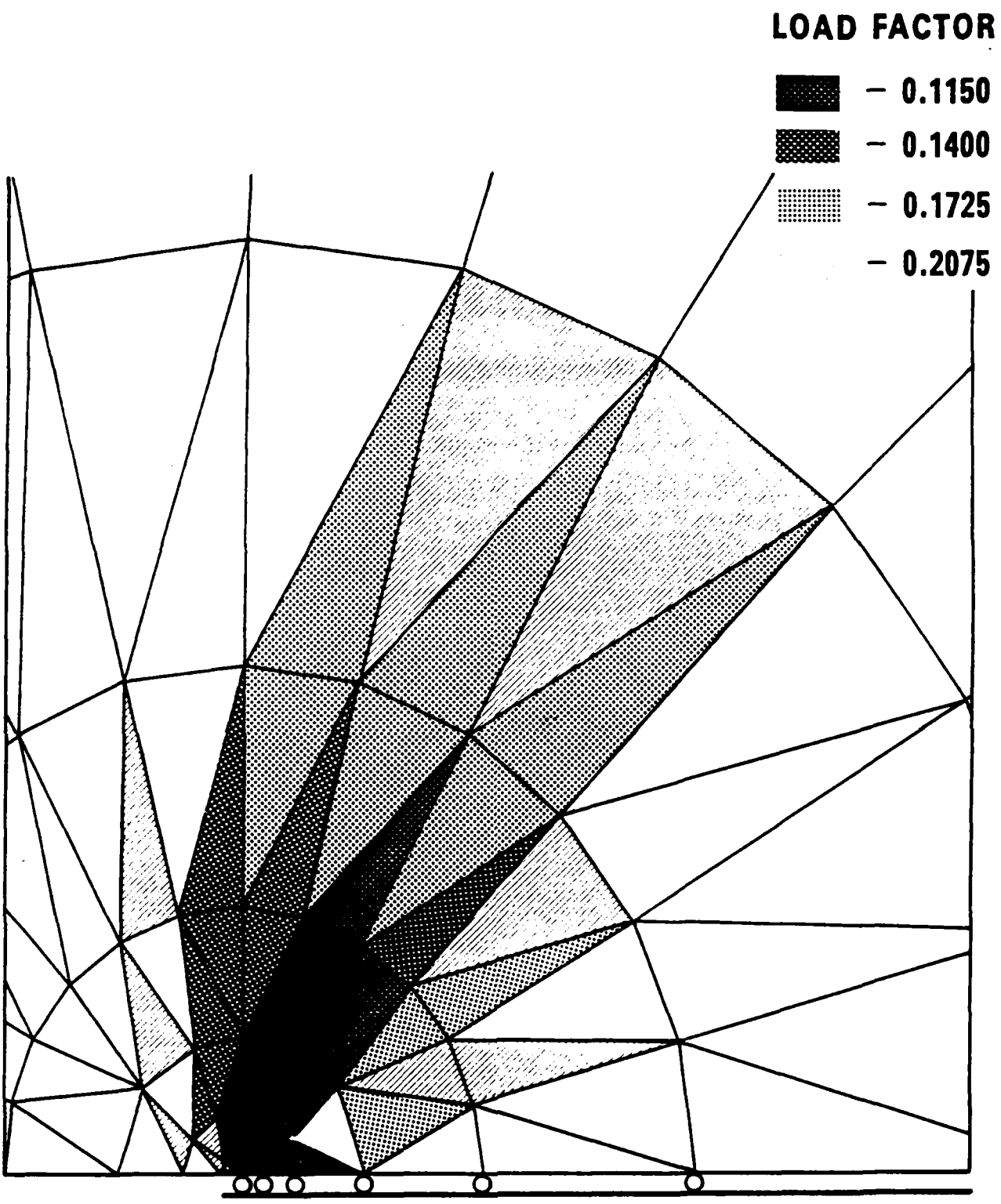

Figure 12. Growth of the Plastic Zone (ADINA)

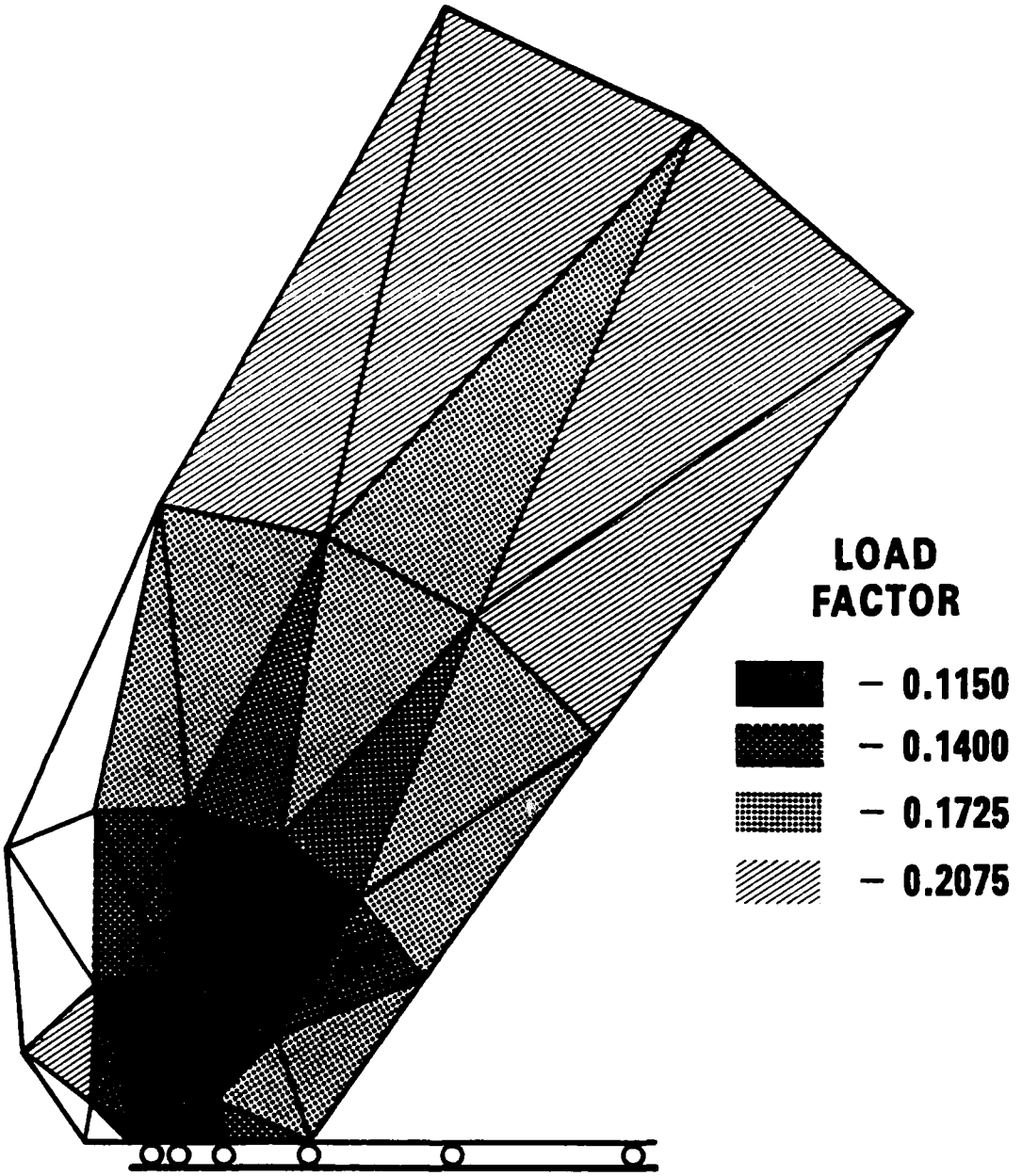

Figure 13. Growth of the Plastic Zone (BIE)

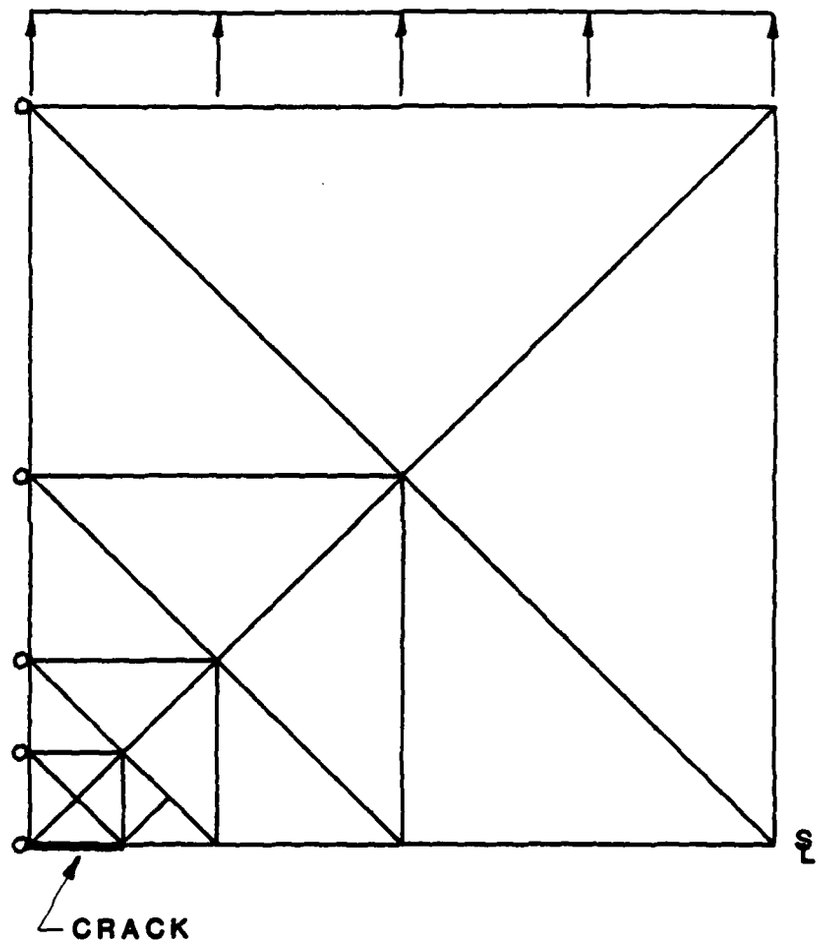

Figure 14. Test Problem for Uniform Strains

Figure 15 shows the final application problem for this study. The model includes a simplified internal mesh for modeling plasticity at a hole in tension. The plate is two units long by one unit wide (W). The hole radius (R) is 0.25W. Local meshes were used to model crack tips at 0.05R and at 0.5R. The elastic KT for this mesh is computed to be 3.29 as compared to 3.24 from Peterson [12]. The elastic stress intensity factors for the two crack lengths are 13% higher than the values given by Rooke and Cartwright [13], which is due to the finite width of the specimen.

Figure 16 shows the progressive generation of the plastic zone at the hole. The material is modeled in plane strain with a yield stress (perfect plasticity) of 50 ksi. The plate is loaded to a level of 44.6 ksi applied at the end of the plate. This level of loading was exaggerated in order to generate a plastic zone that encompassed both crack lengths. In fact, the notch was found to undergo substantial reverse yielding at unloading. After the plastic strains are computed for the notch alone, the crack is introduced through eqs. (6,7). The boundary solution computes crack face closure corresponding to the residual strains. With application of the residual strain and boundary terms, the internal strain algorithm predicts localized reversed plastic flow at the crack tip. Elastic stress intensity factors are computed for the residual terms, without the unloading corresponding to introduction of the crack, and for the residual terms with full unloading of the crack surface.

Table 2 summarizes the numerical results. The engineering approach often used for cracks at notches with prior plasticity is to take the residual strains (and resulting stresses) prior to unloading and to use these as pseudo tractions on the crack faces. This approach corresponds to the second set of results in Table 2, for zero crack surface unloading. The results show that the residual strains produce crack closure (negative stress intensity factor) and a corresponding reduction in the maximum stress intensity factor at load. The effect is, of course, more pronounced for the small flaw as it is more completely buried by the prior plastic zone.

Table 2.

Stress Intensity Factor Results ($KI/\sigma\sqrt{\pi a}$)

	a/R = 0.05	a/R = 0.5
Elastic		
- Max. load	3.411	2.070
- Zero load	0	0
Plastic (Zero Crack Surface Unloading)		
- Max. load	1.483[a]	1.886[a]
- Zero load	-1.928[b]	-0.184[b]
Plastic (Full Crack Surface Unloading)		
- Max. load	0.843[a]	1.787[a]
- Zero load	-2.568[b]	-0.283[b]

Note a: Maximum load values (elastically) = Elastic + Zero load values

Note b: Negative values of K_I imply crack closure at positive load

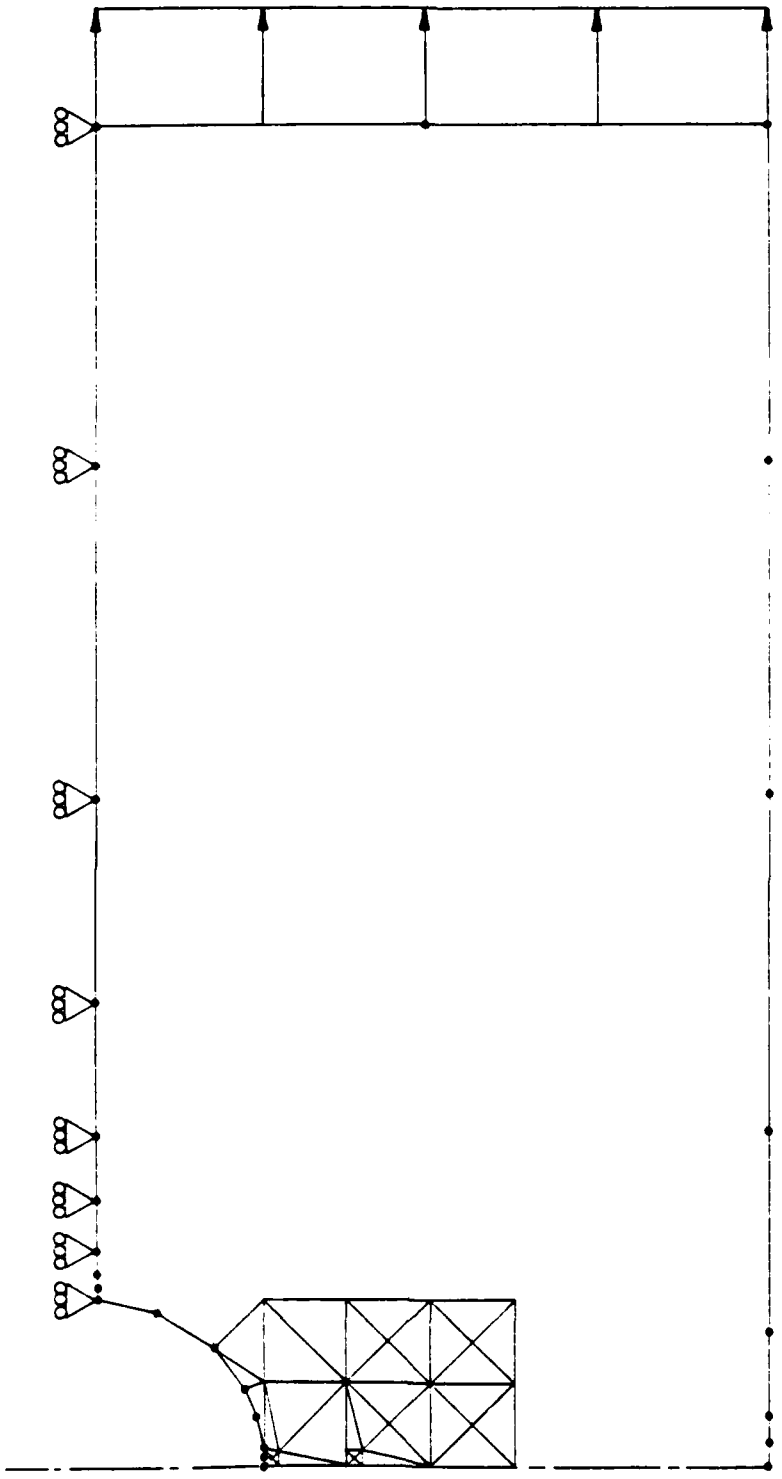

Figure 15. BIE Model of 2:1 Plate with Central Circular Hole (R/W = 00.25)

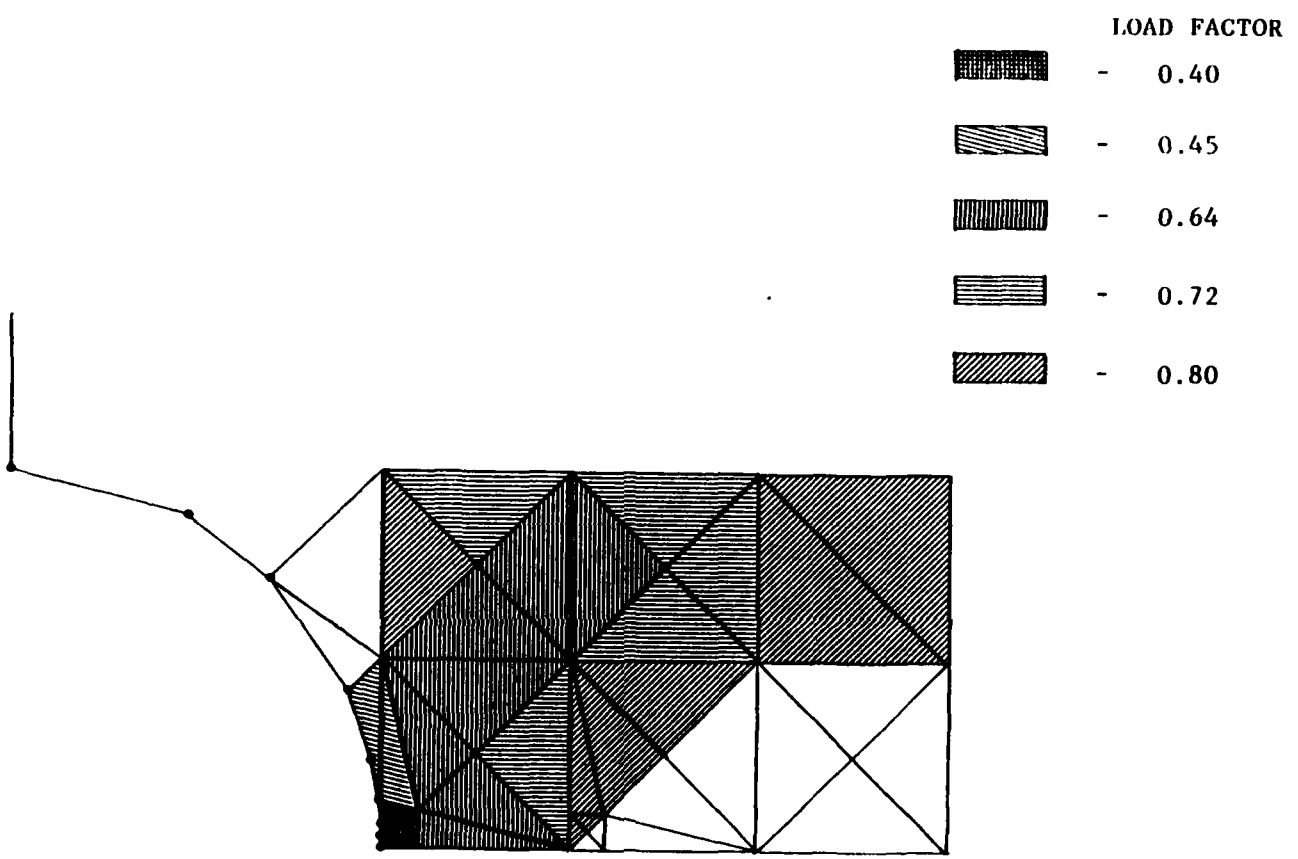

Figure 16. Progressive Generation of Plastic Zone at Hole (Tension Only)

The more correct result for the stress intensity factor calculations is provided by the third set of results in Table 2 with full crack surface unloading. The point to be made is the significant difference between the results assuming no crack face unloading of the residual stresses, and those for full unloading. The usual engineering approaches to modeling crack growth in a notch with plasticity [14, 15] do not account for this unloading, which occurs at positive applied loads (crack open). The effect is most significant for short cracks, which generally consume most of the crack growth life.

The same discrepancy between the engineering and more correct results, including unloading effects, will occur for problems of residual welding strains and thermal gradient strains. The new algorithm presented herein is offered as an effective means for correcting the engineering approach when the plastic zone can be estimated or computed, if not by BIE, then by finite element procedures.

RESEARCH COMMUNICATION

The research to date has involved three individuals. The program manager is Dr. T. A. Cruse. Dr. Arje Nachman was a co-principal investigator on the effort for a few months prior to his taking a position with the Hampton Institute, Hampton, Virginia. Dr. E. Z. Polch, who was developing the computer algorithms for the current research, has been serving as co-principal investigator since that time.

The research results to date have been incorporated in several manuscripts. These include a chapter in a major reference book on BIE, two journal submittals, and two conference proceedings. The following list summarizes these submittals:

1. "Fracture Mechanics," T. A. Cruse, Boundary Element Methods in Mechanics, book in series Computational Methods in Mechanics, edited by D. E. Beskos, Elsevier Science Publishers B.V., Amsterdam, to be published.

2. "Elastoplastic BIE Analysis of Cracked Plates and Related Problems, Part 1: Formulation," T. A. Cruse and E. Z. Polch, submitted to International Journal for Numerical Methods in Engineering.

3. "Elastoplastic BIE Analysis of Cracked Plates and Related Problems, Part 2: Numerical Results," T. A. Cruse and E. Z. Polch, submitted to International Journal for Numerical Methods in Engineering.

4. "Advanced Algorithms for Fracture Mechanics Analysis in Two and Three Dimensions," T. A. Cruse and E. Z. Polch, 2nd International Conference on Variational Methods in Engineering, Southampton, England, July 17-19, 1985.

5. "BIE Analysis of Crack Tip Plastic Zones," T. A. Cruse and E. Z. Polch, AIAA 26th Structures, Structural Dynamics, and Materials Conference, Orlando, Florida, April 15-17, 1985.

The paper from the 26th AIAA Structures, Dynamics, and Materials conference is currently under revision to add some additional information relative to the calculation of crack tip stress intensity factors, including the effects of plasticity. The paper will be submitted shortly to the

International Journal of Fracture and will also be co-authored by Cruse and Polch. The efforts from the second year of the contract will also result in several publication submittals. At this time it is probable that these articles will be submitted for publication in the Engineering Fracture Mechanics Journal and the International Journal of Fracture. Some specific aspects of the current research will be included in further review type articles by Cruse, and in various conference proceedings.

Dr. Cruse has made two trips associated with other business activities which have resulted in specific consultation on the problems of crack growth modeling with elastoplastic models. The current research effort was discussed in detail with Mr. James Rudd of the Air Force Flight Dynamics Laboratory on and with Dr. James Newman of NASA (Langley Research Center). Both individuals expressed interest in this work and will be kept informed of the research progress. A brief telecon was held with Dr. Ted Nicholas to inform him of the principal results of the work and to inform him of the potential for application of the research to the small flaw problem.

REFERENCES

1. Snyder, M. D., and Cruse, T. A., "Boundary-Integral Equation Analysis of Anisotropic Cracked Plates," International Journal of Fracture, vol. 11, 315-328 (1975).

2. Cruse, T. A., "Two Dimensional Boundary-Integral Equation Fracture Mechanics Analysis," Applied Mathematics Modeling, vol. 2, 287-292 (1978).

3. Cruse, T. A., and Polch, E. Z., "Elastoplastic BIE Analysis of Cracked Plates and Related Problems," submitted for publication (1985).

4. Greenberg, M. D., Application of Green's Functions in Science and Engineering, Prentice-Hall, New Jersey (1971).

5. Mukherjee, S., "Corrected Boundary-Integral Equations in Planar Thermoelastoplasticity," International Journal of Solids & Structures, vol. 13, 331-335 (1977).

6. Hutchinson, J. W., "Singular Behavior at the End of a Tensile Crack in a Hardening Material," Journal of Mechanics and Physics of Solids, vol. 16, 13-31 (1968).

7. Stern, M., Becker, E. B., and Dunham, R. S., "A Contour Integral Computation of Mixed-Mode Stress Intensity Factors," International Journal of Fracture, vol. 12, 359-368 (1976).

8. Bathe, K. J., Finite Element Procedures in Engineering Analysis, Prentice-Hall, Inc., Englewood Cliffs, New Jersey (1982).

9. Haward, R. N., and Owen, D. R. J., "The Yielding of a Two Dimensional Void Assembly in an Organic Glass," Journal of Materials Science, vol. 8, pp. 1136-1144 (1973).

10. Telles, J. C. F., The Boundary Element Method Applied to Inelastic Problems, Volume 1 in the series Lecture Notes in Engineering, ed. C.A. Brebbia and S.A. Orszag, Springer-Verlag, Berlin (1983).

11. Larsson, S. G., and Carlsson, A. J., "Influence of Non-Singular Stress Terms and Specimen Geometry on Small-Scale Yielding at Crack Tips in Elastic-Plastic Materials," Journal of the Mechanics and Physics of Solids, vol. 21, pp. 263-277 (1973).

12. Paterson, R. E., Stress Concentration Factors, J. Wiley and Sons, New York, p. 150 (1974).

13. Rooke, D. P., and Cartwright, D. J., Compendium of Stress Intensity Factors, Her Majesty's Stationary Office, London (1976).

14. Grandt, A. F., Jr., and Kullgren, T. E., "Tabulated Stress Intensity Factor Solutions for Flawed Fastener Holes," Engineering Fracture Mechanics, vol. 18, pp. 435-451 (1983).

15. Chang, J. B., "Prediction of Fatigue Crack Growth at Cold-Worked Fastener Holes," Journal of Aircraft, vol. 14, 903-908 (1977).

END

FILMED

1-86

DTIC